

Dispersion of exciton polaritons in cavity-embedded quantum wells

Stefan Jorda

Institut für Theoretische Physik, Universität Regensburg, D-93040 Regensburg, Federal Republic of Germany

(Received 5 December 1994; revised manuscript received 3 January 1995)

We study the interaction of quantum-well excitons with the electromagnetic normal modes of a multilayer dielectric cavity for finite in-plane wave vectors. In the strong-coupling regime we obtain the dispersion of the exciton polaritons by analyzing the exciton spectral function. We compare our numerical results with the recent angle-resolved photoluminescence data by Houdré *et al.* [Phys. Rev. Lett. **73**, 2043 (1994)]. We find a very good agreement for the lower polariton branch and a discrepancy between theory and experiment for the upper polariton branch that is probably due to an experimental inaccuracy.

The investigation of the optical properties of cavity-embedded quantum wells (QW's) has evidenced interesting effects as compared both to simple QW's or to bulk material. In simple QW's, the coupling of the exciton to a continuum of photon states provides an intrinsic mechanism for radiative decay in the radiative region, i.e., where $\omega > cQ_{\parallel}/\sqrt{\epsilon_{\infty}}$, Q_{\parallel} being the in-plane wave vector. The radiative lifetime has been calculated by different methods and the real frequency shift shown to be very small.¹⁻³ In bulk material, in contrast, the exciton couples only to one photon state due to conservation of momentum. As a consequence, no radiative decay takes place but the interaction leads to a large frequency shift responsible for the Rabi or polariton splitting. In microcavities Fabry-Pérot quasimodes emerge out of the photon continuum as the reflectivity of the cavity mirrors increases. The interaction of these quasimodes with the QW excitons follows two different regimes, depending on the design of the cavity and the embedded QW's. Roughly speaking, if the linewidth of the cavity quasimode (determined by the mirror reflectivity) exceeds the interaction energy (determined mainly by the exciton oscillator strength) these structures present enhanced spontaneous emission at an in-plane wave vector Q_{\parallel} determined by exciton and cavity mode resonance.^{4,5} This is the weak-coupling regime. The strong-coupling regime (cavity linewidth smaller than interaction energy) is characterized by a normal-mode (Rabi) splitting between QW excitons and cavity quasimodes, similar to the splitting found for bulk polaritons. However, in contrast to bulk material, the photonic and excitonic properties can be tailored almost independently by the design of the cavity and the embedded QW, respectively. In addition, different experimental techniques can be used in order to bring the exciton and cavity mode into resonance. This has been achieved by probing different spots of a wedge shaped sample,⁶ by taking advantage of the in-plane dispersion of the cavity modes in combination with a wedge shaped sample,⁷ or by the fact that the exciton energy decreases much stronger with increasing temperature than the cavity mode does.⁸ The Rabi splitting corresponds to a time-domain oscillation between the exciton and cavity mode, which has been experimentally detected recently.⁹

Theoretical investigations concerning the interaction of

excitons with cavity modes have been undertaken both by a semiclassical and a quantum approach. Odani *et al.*¹⁰ and Savona *et al.*¹¹ used the semiclassical approach which consists in solving Maxwell's equations with a local¹⁰ or nonlocal¹¹ excitonic susceptibility. An interesting result found in Ref. 11 is that the splittings measured in absorption, reflectivity, transmission, and photoluminescence are, in general, all different, and do not agree with the Rabi splitting. This gets more pronounced as R , the reflectivity of the mirrors, decreases and the nonradiative exciton damping increases. On the other hand, quantum calculations were performed by Citrin,¹² Savona *et al.*,¹¹ and Jorda.¹³ Savona *et al.*¹¹ used an approximate expression for the reflectivity of the cavity mirrors and found an analytic expression for the Rabi splitting assuming resonance of the exciton and cavity mode. In Ref. 13 an expansion of the electromagnetic field in terms of the exact normal modes of the whole space was adopted. This works even for cavities which are almost completely open.¹⁴ It should be noted that as far as only the polariton dispersion is concerned, the semiclassical and the quantum approach are fully equivalent. The quantum approach is however required as a starting point for the investigation of, e.g., polariton squeezing¹⁵ or nonclassical statistical properties of polaritons.¹⁶

In order to describe the angle-resolved photoluminescence data by Houdré *et al.*,⁷ we extend in this paper our previously presented theory,¹³ which was restricted to $Q_{\parallel} = 0$, to the case of finite in-plane wave vector Q_{\parallel} . In the experiment of Ref. 7 a $3\lambda/2$ wide GaAs cavity was sandwiched between two distributed Bragg reflectors (DBR's). The number of periods in the DBR's were chosen different on each side, in order to compensate for the different reflectivities at the outer interfaces to air and to the substrate, respectively. Due to this compensation we restrict our study to a hypothetical symmetrical structure with the substrate on both sides. We could as well choose a structure with air on both sides, the only difference being the appearance of guided modes in the nonradiative region, which is not the subject of this study. In the $3\lambda/2$ cavity two QW arrays were placed at positions where only odd electromagnetic modes have antinodes and interact with the QW excitons. This allows for a reduction of the basis set needed for the expansion of

the vector potential. The solutions of Maxwell's equations in the empty cavity are plane waves in the cavity plane (we choose henceforth $\vec{Q}_{\parallel} \parallel \hat{e}_x$) multiplied by properly matched right and left traveling waves (with respect to the growth direction z) in the individual layers. For $\vec{Q}_{\parallel} \parallel \hat{e}_x$ the electromagnetic TE modes, which interact with the T polarized excitons, are polarized parallel to \hat{e}_y . Then the vector potential can be expanded in terms of creation and annihilation operators for electromagnetic modes ($c_{Q_{\parallel}\rho}^{\dagger}, c_{Q_{\parallel}\rho}$) as

$$A_y(\mathbf{r}) = \sum_{Q_{\parallel}\rho} \left(\frac{2\pi\hbar c^2}{\tilde{\omega}_{Q_{\parallel}\rho} \varepsilon_s \theta \mathcal{A} \mathcal{L}} \right)^{1/2} \times (c_{Q_{\parallel}\rho} e^{iQ_{\parallel}x} + c_{Q_{\parallel}\rho}^{\dagger} e^{-iQ_{\parallel}x}) R(z). \quad (1)$$

The modes with the same Q_{\parallel} but different energy can be distinguished by ρ which corresponds to Q_z in the surrounding medium characterized by the dielectric constant ε_s . $\tilde{\omega}_{Q_{\parallel}\rho} = \sqrt{c^2/\varepsilon_s(Q_{\parallel}^2 + \rho^2)}$ is the frequency of the modes, $R(z)$ is the properly matched linear combination of right and left traveling plane waves, and \mathcal{A} (\mathcal{L}) is a normalization area (length). The normalization constant of the electromagnetic modes θ is given by $|A_s|^2 + |B_s|^2$, where A_s and B_s are the field amplitudes in the surrounding layers.^{13,17} A_s and B_s are related to the amplitudes at the interface central-layer-DBR, A_c and B_c , by a transfer matrix M , which incorporates propagation through the layers as well as the proper boundary conditions at the interfaces. The relation

$$\begin{pmatrix} A_s \\ B_s \end{pmatrix} = M \begin{pmatrix} A_c \\ B_c \end{pmatrix} = \frac{1}{2i} M \begin{pmatrix} \exp(i\phi_c) \\ -\exp(-i\phi_c) \end{pmatrix} \quad (2)$$

holds for odd electromagnetic modes and the phase $\phi_c = \rho_c l_c$ with $\rho_c = \sqrt{\varepsilon_c \rho^2 / \varepsilon_s + (\varepsilon_c / \varepsilon_s - 1) Q_{\parallel}^2}$. ε_c is the dielectric constant of the central layer and l_c half its width. The 2×2 transfer matrix M can be decomposed into contributions from the individual layers and interfaces as^{18,19}

$$M = D_s^{-1} T^N D_c, \quad (3)$$

where N is the number of pairs of quarter-wave layers and the matrix T describes the transmission through one pair of them. T is given by

$$T = D_2 P_2 D_2^{-1} D_1 P_1 D_1^{-1}, \quad (4)$$

with the dynamical matrices D_i and the propagation matrices P_i for the i th layer^{18,19}

$$D_i = \begin{pmatrix} 1 & 1 \\ \frac{c}{\omega} \rho_i & -\frac{c}{\omega} \rho_i \end{pmatrix}, \quad (5)$$

$$P_i = \begin{pmatrix} \exp(i\phi_i) & 0 \\ 0 & \exp(-i\phi_i) \end{pmatrix}. \quad (6)$$

Here ρ_i is defined by an analogous relation as ρ_c and the phases ϕ_i are given by $\phi_i = \rho_i l_i$ with the layer thickness l_i . T is a unimodular matrix and, therefore, the N th power can be evaluated analytically with the help of the Chebyshev identity.^{18,19}

With the expansion (1) the expression for the electro-

magnetic field energy $(1/8\pi) \int (\mathbf{E} \cdot \mathbf{D} + B^2) dV$ reduces to $H_{\text{em}} = \sum_{Q_{\parallel}\rho} \hbar \tilde{\omega}_{Q_{\parallel}\rho} c_{Q_{\parallel}\rho}^{\dagger} c_{Q_{\parallel}\rho}$.

The exciton-photon interaction can be derived from the terms linear and quadratic in the vector potential by the procedure described in Refs. 2 and 14. It yields the expressions

$$H_{\text{int}}^{(1)} = \sum_{Q_{\parallel}\rho} C_{Q_{\parallel}\rho} (c_{Q_{\parallel}\rho} + c_{-Q_{\parallel}\rho}^{\dagger}) (B_{Q_{\parallel}}^{\dagger} + B_{-Q_{\parallel}}), \quad (7)$$

$$H_{\text{int}}^{(2)} = \sum_{Q_{\parallel}\rho\rho'} \frac{C_{Q_{\parallel}\rho} C_{Q_{\parallel}\rho'}}{\hbar \Omega_{\text{ex}}} (c_{Q_{\parallel}\rho}^{\dagger} + c_{-Q_{\parallel}\rho}) (c_{Q_{\parallel}\rho'} + c_{-Q_{\parallel}\rho'}^{\dagger}), \quad (8)$$

where $B_{Q_{\parallel}}^{\dagger}$ ($B_{-Q_{\parallel}}$) is an exciton creation (annihilation) operator and the coupling constant is

$$C_{Q_{\parallel}\rho} = \left(\frac{2\pi\hbar}{\tilde{\omega}_{Q_{\parallel}\rho} \varepsilon_s \theta \mathcal{L}} \right)^{1/2} \mu \Omega_{\text{ex}} \phi(0) O(\rho). \quad (9)$$

Here μ is the dipole matrix element $e \langle c|x|v \rangle$ between the bulk band-edge Bloch states for conduction ($|c\rangle$) and valence band ($|v\rangle$) and Ω_{ex} is the exciton frequency. $\phi(0)$ is the exciton relative function at the vanishing electron-hole separation in the QW. The function $O(\rho)$ is a measure of the overlap between QW subband functions and electromagnetic modes. It will be given explicitly further below.

The Hamiltonian for the coupled exciton radiation system can now be written as

$$H = \sum_{Q_{\parallel}} \hbar \Omega_{\text{ex}} B_{Q_{\parallel}}^{\dagger} B_{Q_{\parallel}} + H_{\text{em}} + H_{\text{int}}^{(1)} + H_{\text{int}}^{(2)}, \quad (10)$$

where we neglect the spatial dispersion of the exciton. In the literature different methods were used to diagonalize exactly Hamiltonian (10). This can be done by solving the Heisenberg equations for the exciton and photon operators,² by the generalized Hopfield transformation,¹⁴ or by summing the Dyson series for the correlation function for the dipole moment.¹² As a result one obtains the dispersion relation for the coupled exciton-photon excitations

$$\hbar^2(\omega^2 - \Omega_{\text{ex}}^2) - 2\hbar\Omega_{\text{ex}} \Sigma(\omega) = 0, \quad (11)$$

with the exciton self-energy

$$\Sigma(\omega) = \frac{\omega^2}{\Omega_{\text{ex}}^2} \sum_{\rho} \frac{2\tilde{\omega}_{Q_{\parallel}\rho} |C_{Q_{\parallel}\rho}|^2}{\hbar[(\omega + i\delta)^2 - \tilde{\omega}_{Q_{\parallel}\rho}^2]} O^2(\rho). \quad (12)$$

The real part of the self-energy is

$$\begin{aligned} \text{Re} \Sigma(\omega) &= -\frac{4\mu^2 \omega^2}{c^2} \phi^2(0) \\ &\times \int_0^{\infty} \frac{d\rho}{\rho^2 + Q_{\parallel}^2 - \varepsilon_s \omega^2 / c^2} \frac{1}{\theta} O^2(\rho), \end{aligned} \quad (13)$$

and the imaginary part

$$\text{Im} \Sigma(\omega) = \frac{2\pi\mu^2 \omega^2}{c^2 \rho_s} \frac{1}{\theta} \phi^2(0) O^2(\rho). \quad (14)$$

Instead of solving Eq. (11) numerically for complex frequency we determine the polariton energy by the analysis of the appropriate spectral function as a function of real ω . This spectral function is the imaginary part of the correlation function for the dipole moment.¹² For $\omega \approx \Omega_{\text{ex}}$ it reduces to the exciton spectral function, given by²⁰

$$A^{\text{ex}}(\omega) = -2 \text{Im} G^{\text{ret}}(\omega) \propto \frac{\text{Im} \Sigma(\omega)}{[\omega - \Omega_{\text{ex}} - \text{Re} \Sigma(\omega)]^2 + [\text{Im} \Sigma(\omega)]^2}, \quad (15)$$

where $G^{\text{ret}}(\omega)$ is the retarded exciton Green's function. Using the rotating wave approximation would have lead directly to the exciton spectral function. The polariton energy is determined by the maxima in the spectral function.

The sample of Ref. 7 consists of two QW arrays, each comprising three approximately $L = 75 \text{ \AA}$ wide $\text{In}_{0.13}\text{Ga}_{0.87}\text{As}$ QW's. These QW's are $L_B = 100 \text{ \AA}$ apart and the two arrays placed a distance $\lambda/2$ away from the interfaces inside a $3\lambda/2$ wide GaAs cavity. The DBR at the substrate side is made of 19 pairs of alternating AlAs and $\text{Al}_{0.1}\text{Ga}_{0.9}\text{As}$ layers of width $\lambda/4$. The whole structure is wedge shaped leading to a different energetic position of the QW exciton and cavity mode across the sample. For the numerical calculations we used the values (for $\hbar\omega = 1.3 \text{ eV}$) $\varepsilon_c = \varepsilon_s = 12.53$ (GaAs), $\varepsilon_1 = 8.76$ (AlAs), $\varepsilon_2 = 12.15$ ($\text{Al}_{0.1}\text{Ga}_{0.9}\text{As}$).²¹ The heavy-hole exciton oscillator strength f , which is related to the quantities μ and $\phi(0)$ by $\mu^2 \phi^2(0) = (\hbar e^2 / 2m E_g) f$, was calculated by solving the momentum-space two-particle Schrödinger equation including light-hole-heavy-hole mixing with a modified quadrature method.²² A value of $f = 52 \times 10^{-5} \text{ \AA}^{-2}$ was found. The function $O^2(\rho)$, which is a measure of the overlap between electromagnetic field and the QW's, is given by

$$O^2(\rho) = 2 \sum_{k=-1}^{+1} \cos^2 \left[\rho_c \left(\frac{l_c}{3} + k(L + L_B) \right) \right], \quad (16)$$

where ρ_c has to be expressed in terms of ρ . In deriving Eq. (16) the coupling between excitons in different QW's was neglected.²³

In Figs. 1–3 we present numerical results for the polariton dispersion for different resonance conditions of the exciton and cavity mode, corresponding to the conditions of Fig. 3 in Ref. 7. As we have no knowledge of the widths of the individual layers at the investigated spots of the sample, we adjusted the exciton energy and the cavity mode energy at $Q_{\parallel} = 0$ in order to fit as good as possible the experimental result at $Q_{\parallel} = 0$. Due to the high-reflectivity mirrors (and corresponding small linewidth of the cavity mode) and the fact that there are several QW's embedded in the cavity, the influence of the nonradiative exciton damping [which can be easily introduced phenomenologically in Eq. (15)] is not important. As a consequence, the polariton dispersion can be compared directly to the photoluminescence signal.¹¹ We see that, whereas the dispersion of the lower polariton branch agrees well with the experimental result (shown as squares), there appears a discrepancy between the

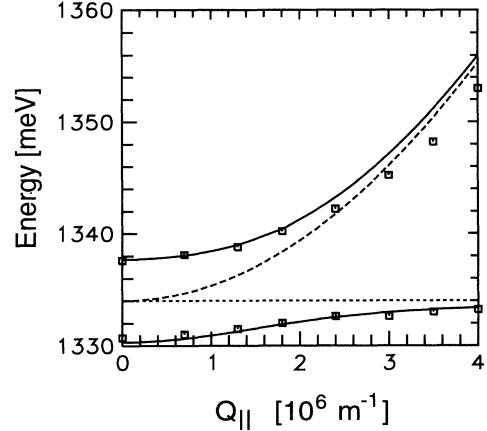


FIG. 1. Polariton dispersion (full lines) in the case of coinciding exciton and cavity mode energy at $Q_{\parallel} = 0$. The exciton (cavity mode) energy is shown as dotted (dashed) line. The squares show the experimental points of Fig. 3(a) in Ref. 7.

ory and the published experimental data for the upper branch. This seems to be due to the dispersion of the cavity mode (shown as dashed line) determined theoretically by the complex zeros of θ or by an analysis of the bare photon spectral function, which is proportional to $1/\theta$.¹³ The dispersion of the cavity mode can be described by the relation

$$\Omega(Q_{\parallel}) = \sqrt{\Omega(0)^2 + \frac{c^2 Q_{\parallel}^2}{n_{\text{eff}}^2}}, \quad (17)$$

where the effective index of refraction n_{eff} is an average of the refractive indices of the different layers. Due to the field penetration into the DBR's n_{eff} is always smaller than n_c . By comparison with the numerical calculation we find a value $n_{\text{eff}} = 3.26$, very close to the value $n_{\text{eff}} = \sqrt{n_1 n_2} = 3.24$ derived by Pidgeon and Smith²⁴ for the case $n_c = n_2 > n_1$ in a $\lambda/2$ cavity. From the experimental data of Ref. 7 a value as high as $n_{\text{eff}} \approx n_c \approx 3.5$ can be extracted, which is a surprising result, as it cannot be obtained theoretically within the limits imposed by the experimental determination of the refractive indices of GaAs and AlAs. The authors of Ref. 7 also present

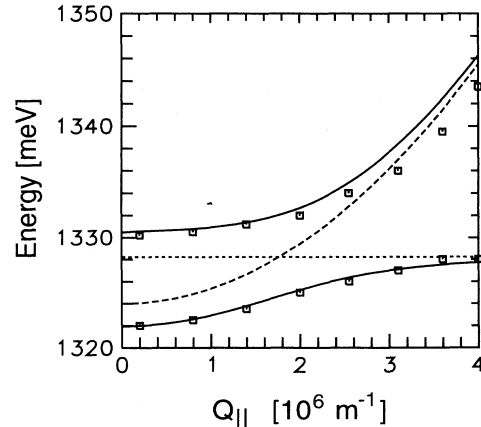


FIG. 2. Same as Fig. 1 for different resonance conditions, corresponding to Fig. 3(b) of Ref. 7.

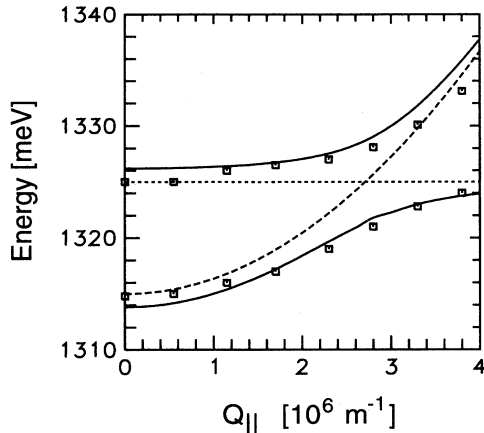


FIG. 3. Same as Fig. 1 for different resonance conditions, corresponding to Fig. 3(c) of Ref. 7.

semiclassical calculations based on a Lorentz oscillator in a cavity formed by DBR mirrors. The same values for the refractive indices of GaAs and AlAs as in the present paper are used and for the dispersion of the cavity mode Eq. (17) is cited. However, although not stated explicitly,

n_{eff} was used as a fitting parameter in order to get the best agreement between theory and experiment.²⁵ The origin of the discrepancy between the experimental data and our calculations is probably due to an experimental uncertainty in the angular measurement. The difference between theory and experiment corresponds to an angle error of about $2^\circ - 3^\circ$, which seems reasonable according to the experimental setup.²⁵

In conclusion, we have presented a quantum theory for the coupled exciton-photon excitations in cavity-embedded QW's that is based on an expansion of the uncoupled electromagnetic field in terms of normal modes of the whole space. The in-plane dispersion of the two polariton branches in the strong-coupling regime was obtained and compared to available experimental data. We have commented on the apparent discrepancies between theory and experiment which arise probably due to the experimental difficulty of determining the angles exactly enough.

I am grateful to R. Winkler for the calculation of the oscillator strength. Thanks are also given to R. Houdré, R.P. Stanley, and V. Savona for providing preprints of their papers prior to publication and for clarifying discussions.

- ¹ F. Tassone, F. Bassani, and L.C. Andreani, *Nuovo Cimento D* **12**, 1673 (1990); *Phys. Rev. B* **45**, 6023 (1992).
- ² S. Jorda, U. Rössler, and D. Broido, *Phys. Rev. B* **48**, 1669 (1993); *Superlatt. Microstruct.* **12**, 85 (1992).
- ³ D.S. Citrin, *Phys. Rev. B* **47**, 3832 (1992).
- ⁴ N. Ochi, T. Shiotani, M. Yamanishi, Y. Honda, and I. Suenune, *Appl. Phys. Lett.* **58**, 2735 (1991).
- ⁵ Y. Yamamoto, S. Machida, Y. Horikoshi, K. Igeta, and G. Björk, *Opt. Commun.* **80**, 337 (1991).
- ⁶ C. Weisbuch, M. Nishioka, A. Ishikawa, and Y. Arakawa, *Phys. Rev. Lett.* **69**, 3314 (1992).
- ⁷ R. Houdré, C. Weisbuch, R.P. Stanley, U. Oesterle, P. Pelandini, and M. Ilegems, *Phys. Rev. Lett.* **73**, 2043 (1994).
- ⁸ T.A. Fisher, A.M. Afshar, D.M. Whittaker, M.S. Skolnick, J.S. Roberts, G. Hill, and M.A. Pate, *Phys. Rev. B* **51**, 2600 (1995).
- ⁹ T.B. Norris, J.-K. Rhee, C.-Y. Sung, Y. Arakawa, M. Nishioka, and C. Weisbuch, *Phys. Rev. B* **50**, 14 663 (1994).
- ¹⁰ K. Odani, Y. Ohfuti, and K. Cho, *Solid State Commun.* **87**, 507 (1993). Although not explicitly emphasized, a different splitting in absorption and reflectivity was already obtained in this paper.
- ¹¹ V. Savona, L.C. Andreani, P. Schwendimann, and A. Quattropani, *Solid State Commun.* **93**, 733 (1995).
- ¹² D.S. Citrin, *IEEE J. Quantum Electron.* **QE-30**, 997 (1994).
- ¹³ S. Jorda, *Phys. Rev. B* **50**, 18 690 (1994). The value for the oscillator strength given in this paper is incorrect. It should be $f = 65 \times 10^{-5} \text{ \AA}^{-2}$.
- ¹⁴ S. Jorda, *Phys. Rev. B* **50**, 2283 (1994).
- ¹⁵ M. Artoni and J.L. Birman, *Phys. Rev. B* **44**, 3736 (1991).
- ¹⁶ P. Schwendimann and A. Quattropani, *Europhys. Lett.* **17**, 355 (1992).
- ¹⁷ D. Marcuse, *Theory of Dielectric Optical Waveguides* (Academic Press, New York, 1974).
- ¹⁸ M. Born and E. Wolf, *Principles of Optics* (Pergamon Press, Oxford 1970).
- ¹⁹ P. Yeh, *Optical Waves in Layered Media* (John Wiley & Sons, New York, 1988).
- ²⁰ G.D. Mahan, *Many-Particle Physics* (Plenum Press, New York, 1990).
- ²¹ *Properties of Aluminium Gallium Arsenide*, edited by S. Adachi (INSPEC, The Institution of Electrical Engineers, London, 1993).
- ²² R. Winkler, S. Jorda, and U. Rössler, *Proceedings of the 22nd International Conference on the Physics of Semiconductors, Vancouver, 1994* (World Scientific, Singapore, in press).
- ²³ D.S. Citrin, *Solid State Commun.* **89**, 139 (1994).
- ²⁴ C.R. Pidgeon and S.D. Smith, *J. Opt. Soc. Am.* **54**, 1459 (1964).
- ²⁵ R. Houdré and R.P. Stanley (private communication).